Published in final edited form as:
Cancer Res. 2014 March 1; 74(5): 1329–1337. doi:10.1158/0008-5472.CAN-13-3014.

Fragmented sleep accelerates tumor growth and progression through recruitment of tumor-associated macrophages and TLR4 signaling

Fahed Hakim[1], **Yang Wang**[1], **Shelley XL Zhang**[1], **Jiamao Zheng**[1], **Esma S. Yolcu**[2], **Alba Carreras**[1], **Abdelnaby Khlayfa**[1], **Haval Shirwan**[2], **Isaac Almendros**[1], and **David Gozal**[1]

[1] Pediatric Sleep Medicine, Department of Pediatrics, Comer Children's Hospital, The University of Chicago, Chicago, IL

[2] Department of Microbiology and Immunology, The University of Louisville, Louisville, KY

Abstract

Fragmented sleep (SF) is a highly prevalent condition and a hallmark of sleep apnea, a condition that has been associated with increased cancer incidence and mortality. In this study, we examined the hypothesis that SF promotes tumor growth and progression through pro-inflammatory TLR4 signaling. In the design, we compared mice that were exposed to SF one week before engraftment of syngeneic TC1 or LL3 tumor cells and tumor analysis three weeks later. We also compared host contributions through the use of mice genetically deficient in TLR4 or its effector molecules MYD88 or TRIF. We found that SF enhanced tumor size and weight compared to control mice. Increased invasiveness was apparent in SF tumors, which penetrated the tumor capsule into surrounding tissues including adjacent muscle. Tumor-associated macrophages (TAM) were more numerous in SF tumors where they were distributed in a relatively closer proximity to the tumor capsule, compared to control mice. Although tumors were generally smaller in both MYD88−/− and TRIF−/− hosts, the more aggressive features produced by SF persisted. In contrast, these more aggressive features produced by SF were abolished completely in TLR4−/− mice. Our findings offer mechanistic insights into how sleep perturbations can accelerate tumor growth and invasiveness through TAM recruitment and TLR4 signaling pathways.

Introduction

In recent years, the possibility that sleep duration and overall sleep characteristics may affect overall cancer outcomes has been advanced (1). Indeed, in several epidemiologic studies spanning the last decade the presence of altered sleep duration, both shortened and prolonged sleep, has been associated with higher incidence or adverse prognosis for several solid tumors. (2-17) However, although the role of the circadian clock system in tumorigenesis has been extensively explored (18, 19), no animal models have thus far

Corresponding author: David Gozal, MD, Department of Pediatrics, University of Chicago, 5721 S. Maryland Avenue, MC 8000, Suite K-160 Chicago, IL 60637, USA. Tel: (773) 702-6205; Fax: (773) 702-4523; dgozal@uchicago.edu.

Conflict of Interest: The authors have no conflict of interest to declare in relation to this manuscript.

examined whether the association between disrupted sleep and tumorigenesis is indeed recapitulated, and if so, what potential mechanisms may underlie such associations.

In this context, some efforts to explore causal associations between a highly prevalent sleep disorder, namely obstructive sleep apnea (OSA), and cancer have also taken place (20, 21), and have operated under the assumption that the intermittent hypoxemia that characterizes OSA patients during their sleep period is likely to mimic the biologic events that drive tumor growth(1, 22-27).The major findings from these initial studies indicate that the periodic oscillations in overall oxygenation during sleep in OSA patients impose overall adaptive changes in the tumor metabolic cellular substrate that enhances their proliferative and invasiveness properties (28). However, these studies failed to explore another hallmark characteristic of OSA, namely sleep fragmentation (SF), i.e., the presence of recurrent arousals aimed at restoring airflow that lead to sleep discontinuity.

Using a similar logical paradigm, we hypothesized that chronic SF, a very frequent occurrence in many human disorders, including OSA, would be associated with altered solid tumor proliferation and invasiveness in a murine model (29, 30). Furthermore, we posited that sustained SF would promote changes in the phenotypic distribution of tumor associated macrophages (TAM). Indeed, TAM have been identified as critically important constituents of cancer micro-environment, and are major contributors to cancer progression by releasing a vast array of growth factors, cytokines, inflammatory mediators, and proteolytic enzymes that underlie key components of tumor growth and invasion (31, 32).

Materials and Methods

Animals

Male C57/B6, TLR4−/−, MYD88−/− and TRIF−/− mice weighing ~25 g, were purchased from Jackson Laboratories (Bar Harbor, Maine), housed in a 12 hr light/dark cycle (light on 7:00 am to 7:00 pm) at a constant temperature (24 ± 1°C) and allowed access to food and water *ad libitum*. The experimental protocols were approved by the Institutional Animal Use and Care Committee and are in close agreement with the National Institutes of Health Guide in the Care and Use of Animals. All efforts were made to minimize animal suffering and to reduce the number of animals used.

Sleep Fragmentation

The custom-designed sleep fragmentation approach used to induce SF in rodents has been previously reported in detail (29, 33), and relies on automated intermittent tactile stimulation of freely behaving mice in a standard laboratory mouse cage, using a near-silent motorized mechanical sweeper. This method obviates the need for human contact and intervention, and does not involve introduction of foreign objects or touching of the animals during sleep. To induce sleep fragmentation, we chose a 2-min interval between each sweep, implemented during the light period (7:00 a.m. to 7:00 p.m.). Of note, 4-5 mice were housed in each cage to prevent isolation stress.

Tumor Cell Lines And Culture Medium

We used TC-1 cells (ATCC CRL- 2785) and 3LLC (ATCC CRL-1642) in all experiments. Both cell lines are derived from primary lung epithelial cells of C57/B6 mice and were cultured at 37°C, 95% air, 5% CO2 incubator in full tumor medium as recommended by the American Type Culture Collection (ATCC, Rockville, MD, USA). TC-1 cells were cultured in RPMI 1640 medium with 2 mM L-glutamine adjusted to contain 1.5 g/L sodium bicarbonate, 10 mM HEPES, and 1.0 mM sodium pyruvate supplemented with 2 mM non-essential amino acids, penicillin and streptomycin and 10% fetal bovine serum, all supplied by Gibco, Life Technologies (Grand Island, NY, USA), and selected. with G418 (Gibco, Life Technologies, Grand Island, NY, USA) and Hygromycin B (Calbiochem, EMD Millipore Corporation, Billerica, MA, USA). 3LL cells were cultured in Dulbecco's modified Eagle's medium (DMEM) supplemented with 10% fetal bovine serum (FBS), L-glutamine, penicillin and streptomycin, all supplied from (Gibco, Life Technologies, Grand Island, NY, USA). Study mice were inoculated with TC-1 or 3LL cells [1×10^5 cells in 0·2 ml phosphate-buffered saline (PBS)] by subcutaneous injection into the right lower flank or right thigh for selected experiments.

Tumor Model

All mice strains, both in SC and SF were housed at the same environmental conditions in the same cages. After 7 days of exposures, both SF and SC mice were inoculated with TC-1 or 3LLC cells and tumor growth was monitored 2–3 times per week using a precision caliper. Average tumor size was calculated by measuring two perpendicular diameters. Under these conditions, all the mice develop palpable tumors within 9–12 days. Animals bearing tumors were euthanized at day 28 after injection; tumors were enucleated, scaled, and subjected to different experiments.

Matrix Metalloproteinase (MMP) In Vivo Live Imaging

Twelve C57/B6 male mice (6 SF and 6 SC) were injected subcutaneously with 1×10^5 live TC1 cells into the lateral aspect of the right thigh using the same protocol previously described, 28 days after tumor cell inoculation, mice were intravenously injected with 2 nmoles of the matrix metalloproteinase (MMP) probe MMPSense™ 750 FAST (PerkinElmer, Product number: NEV10168), this MMP activatable agent is optically silent upon injection and produces fluorescent signal after cleavage by disease related MMP's. Activation can occur by a broad range of MMP's including MMP 2, 3, 7, 9, 12, and 13. Two days before the MMPSense injection, all the fur lining the tumor area was removed by hair removal cream, after which mice were imaged 6, 12 and 24 hours post injection using the Xenogen IVIS Spectrum (Perkin Elmer) at the University of Chicago Optical Imaging Core Facility. The tumor near infrared fluorescence (average radiant efficiency) of images was quantified using Living Image Software (Perkin Elmer).

Local Tumor Invasiveness

To assess differences in local tumor invasiveness between the SF and SC groups, 7 days after SF/SC initiation, C57/B6 mice were injected subcutaneously with TC1 cells into the lateral aspect of the right thigh using 1×10^5 cells in 0·2 ml PBS. 28 days after tumor cell

inoculation, both SF and SC mice were euthanized and subjected to wide resection of the tumor tissue with its adjacent muscular and bone tissue of the thigh. The whole specimen was fixed in 4% PFA after it was cut into equivalent size pieces. Those specimens were embedded in paraffin and followed by cutting of 3-5 μm sections and were stained with H&E.

Analysis of tumor infiltrating cells

Tumors were mechanically disrupted in small pieces and maintained overnight in TC1 complete growth medium but without geneticin (G418). After 12 h, cells were harvested and filtered through a 100 μM nylon mesh cell strainer (352350, BD Falcon, Bedford, MA, USA). Prior to cell identification, viable cells were selected by using the aqua-fluorescent reactive dye (L34957, Invitrogen, Eugene, OR, USA). TAM were defined as CD45+, CD11b+, F4/80+ cells.

Isolation of TAM

Tumors were mechanically disrupted and incubated in collagenase IV solution 1mg/mL for 1h at 37°C. Cells were filtered through a 100 μM nylon mesh cell strainer and CD11b+ cells were isolated by magnetic labeling following manufacturer's procedure (EasySep™ Mouse CD11b Positive Selection Kit, StemCell, 18770, Vancouver, BC, Canada).

Immunofluorescence Analysis

Tumors were excised, frozen in OCT and stored in −80 °C. 10 μm cryo-sections were done and stained for F4/80. Sections were washed several times in PBS, and blocked with a PBS/0.4% Triton X-100/0.5% TSA (Tyramide Signal Amplification, Perkin Elmer Life Sciences, Boston, MA) blocking reagent/10% normal horse serum for 1 hour. Sections were then serially incubated with a rabbit anti-mouse F4/80 antibody (1:500; cat# 122604, Biolegend San Diego, CA) at 4°C for 24 h, and then washed in PBS six times for 5 min each wash. Sections were incubated at room temperature for 1 hour in biotinylated antibody (1:400, Vector Labs, Burlingame, CA) in a PBS/0.4% TSA blocking reagent/10% horse serum solution, and then with streptavidin-horseradish peroxidase diluted 1:100 in PBS/0.5% TSA blocking reagent. Subsequently, the sections were incubated with TSA fluorescein reagents diluted 1:50 in amplification diluent (Perkin Elmer Life Sciences) for 2 min. Sections were then washed and mounted onto glass slides. Sections were visualized using a fluorescent microscope by an investigator who was blinded to the sample source.

Endocan Staining

Paraffin sections of SC and SF tumor tissue were stained immunohistochemically for endocan using Anti-mouse Endocan (cat# LIA-0905; Lunginnov, Lille , France) as recommended by the manufacturer.

Total RNA Isolation and Gene Expression

Sorted TAM were instantly frozen in liquid nitrogen after counting the amount of sorted cells. Total RNA was isolated using automated RNA extraction (Promega, Madison, WI) and DNase treated according to manufacturer's protocol. The RNA quantity and integrity

were determined using a Nanodrop Spectrophotometer and Agilent 2100 Bioanalyzer Nano 6000 Lab Chip assay (Agilent Technologies, Santa Clara, CA). Quantitative real-time PCR (QRT-PCR) was performed using the ABI 7500 instrument (Applied Biosystems, Foster City, CA). Complementary DNA was synthesized using a High-Capacity cDNA Archive Kit (Applied Biosystems, Foster City, CA). Five hundred nanograms (500 ng) of total RNA from both SF and SC samples were used to generate cDNA templates for RT-PCR .TaqMan® Master Mix Reagent Kit (Applied Biosystems, Foster City, CA) was used to amplify and quantify the transcripts in 20 μl reactions. Duplicate PCR reactions were performed in 96-well in parallel with the β-actin rRNA as a house keeping gene. The steps involved in the reaction program included: the initial step of 2 minutes at 50°C; denaturation at 95°C for 10 min, followed by 45 thermal cycles of denaturation (15 seconds at 95°C) and elongation (1 min at 60°C). Expression values were obtained from the cycle number (Ct value) using the Biosystems analysis software. These Ct values were averaged and the difference between the β-actin Ct (Avg) and the gene of interest Ct (Avg) was calculated (Ct-diff). The relative gene expression was analyzed using the $2^{-\Delta\Delta CT}$ method. Quantitative results were expressed as the mean ±standard deviation (SD). The following Taqman primer and probes were purchased from Applied Biosystems (Foster City, CA): IL12β assay# Mm00434174_m1, iNOS assay# Mm00440502_m1, INF-γ assay# Mm01168134_m1, Arginase1 assay# Mm00475988_m1, Resistin like Alpha (Fizz1) assay# Mm00445109_m1, Mrc1 assay# Mm00485148_m1, IL10 assay# Mm00439614_m1, TGF-β assay# Mm01178820_m, TRL2 assay#Mm00442346_m1, TLR4 assay# Mm00445273_m1, TLR6 assay# Mm02529782_s1.

Statistical analysis

All data are reported as mean ± SE. Comparisons for tumor growth and all other time course experiments among SF and SC conditions were performed using one-way ANOVA followed by unpaired Student's T-test with Bonferroni correction. Comparison of all other quantitative data between SF and SC conditions was performed using unpaired Student's T-tests. For all comparisons, a p value <0.05 was considered as statistically significant.

Results

SF induces accelerated tumor size growth

C57/B6 mice exposed to SF starting 1-week prior to flank injection with TC-1 cells showed accelerated tumor size growth with significant differences emerging at day 23 following injection and thereafter when compared to mice under control sleep conditions (SC) (Figure 1A; n=53/group; SF vs. SC: p< 0.007). Tumor weight was significantly higher at day 28 in SF-exposed mice (SF-57/B6: 1.955± 0.680 g vs. SC-C57/B6: 1.046±0.479 g; p<0.001). Similarly, mice (n=15/group) exposed to SF and injected with 3LLC cells showed significantly accelerated tumor growth (p<0.001) and tumor weight (p<0.027) compared to SC conditions (SF-57/B6: 1.22 ± 0.281 g vs. SC-C57/B6: 0.543 ±0.163 g; p<0.027-Figure 1B).

SF induces increased tumor invasiveness

When TC-1 cells were injected s.c in the thigh area, increased invasiveness was apparent in SF-C57/B6 tumors compared to SC-C57/B6 tumors, with obvious penetration of surrounding tumor capsule and extension/infiltration into adjacent muscle (Figure 2A; n=12/group; Chi-Square: $p<0.001$). To further explore the increase invasiveness of tumors in SF-exposed mice, we performed live MMP imaging, which showed significantly increased MMP activity in SF-C57/B6 tumors vs. CS-C57/B6 (n=6, $p<0.01$- Figure 2B).

Tumor associated macrophage (TAM) counts and distribution

When compared to CS-C57/B6 tumors, significant increases in TAM counts occurred in SF-C57/B6 tumors whether expressed as TAM/gram tumor tissue (Figure 3A; $p<0.01$) or as TAM/ whole tumor (Figure 3B; $p< 0.01$). TAM in SF-C57/B6 tumors were preferentially distributed in close proximity to the tumor capsule, as compared to increased tumor core location in tumors from SC-C57/B6 mice (Figure 3D & E). When endocan staining was used to identify new vessel formation in the tumor capsule, SF-C57/B6 tumors had higher expression of endocan when compared with SC condition (Figure 3F).

SF induces TAM polarity shift toward M2 and higher TLR4 expression

To further understand whether changes in macrophage polarity occurred during SF, we performed FACS of tumors for TAM (i.e., CD45+ CD11b+ F4/80+) and further assessed the proportion of those expressing CD 86^{high}, a M1 marker or CD 206^{high}, a M2 marker. A shift toward increased M2 marker expression in TAM of SF-C57/B6 tumors emerged, particularly in peripheral areas of the tumor ($p<0.04$; Figure 4A). TAM shift in polarity in SF tumors was also apparent based on increased transcriptional expression of M2 markers when compared to SC conditions, as evidenced by higher expression of Fizz1, Arg1 and Mrc1 ($p<0.01$; Figure 4B). TAM from SF-exposed mice also expressed higher levels of TLR4 compared to SC-exposed mice ($P<0.02$; Figure 4C), but no changes in TLR2 or TLR6 were apparent (data not shown). Based on such findings, we examined TLR4 signaling as a potential pathway mediating SF-induced differences in tumorigenesis as described heretofore.

TLR4 signaling mediates SF-induced tumor progression

When compared to CS-C57/B6 mice, significant reductions in tumor size and weight occurred in SC-TLR4−/− mice ($p<0.001$; Figure 4D and 4E). More interestingly, the accelerated growth and increases in size induced by SF were completely abrogated in SF-TLR4−/− mice (Figure 4D and 4E; $p<0.05$ vs. SC-TLR4−/− mice). These effects were accompanied by significant reductions in TAM count in SF-TLR4−/− mice ($p< 0.01$; Figure 4F). These results prompted further exploration as to whether TLR4 major downstream signaling pathways, namely MYD88 or TRIF were particularly and specifically recruited in SF. As shown in Figure 4G, tumors enucleated from SF-MYD88−/− and SF-TRIF−/− mice showed reductions in tumor weight compared to SF-C57/B6 ($p< 0.03$, $p<0.01$ respectively), but were still significantly larger than in SF-TLR4−/− mice. In addition, small, albeit statistically significant differences between SF and SC for MYD88 and TRIF null mice remained.

Discussion

This study shows that chronically fragmented sleep, a highly prevalent condition associated with a multiplicity of human disorders, leads to accelerated tumor growth and invasiveness in mice and that such adverse effects are mediated, at least in part, by changes in TAM polarity and TLR4 signaling. Indeed, increases in M2 macrophage markers were apparent in tumors of SF-exposed mice, and were accompanied by increased in vivo and in vitro matrix metalloproteinase activity (34, 35). We further show that similar to previous reports, TLR4 signaling not only underlies significant components of tumor progression (34, 35), but also appears to mediate the differences in tumor proliferation between SF and SC conditions. Taken together, these findings provide initial, yet conclusive support for sleep-mediated modulation of tumorigenesis, and suggest that host-dependent immune mechanisms constitute a major pathway of such modulatory influences.

The paramount observation of the present study is the increased tumor proliferation and marked changes in invasiveness induced by chronic SF exposures mimicking several sleep disorders. As such, these observations provide initial observations in a murine model on the effects of perturbed sleep on cancer biology. Furthermore, our study offers potential biological plausibility to some of the findings derived from cross-sectional cohorts that have identified epidemiological associations between perturbed sleep or reduced sleep duration to the incidence and overall outcomes of cancer (2-17). Thus, by establishing the biological plausibility of sleep as a modulator of the intrinsic properties of cancerous tumors, the rationale for further well-controlled epidemiological and intervention studies is warranted. Furthermore, current findings establish a unique murine model that should allow for delineation of the generalizability of SF-induced TC1 and 3LLC tumor property modifications to other solid and non-solid clinically-relevant tumors, and further enable exploration of specific changes in the biological properties of specific cellular components within each of such tumors. In addition, this experimental paradigm will not only permit identification of factors involved in tumor proliferation and invasion, but may also facilitate the investigation of whether sleep perturbations alter metastatic potential and tumor resistance to therapeutic regimens.

The mechanisms mediating the increased tumor proliferative rates induced by implementation of SF are unclear and likely diverse. Importantly, SF-induced effects occurred in both TC-1 and 3LLC tumors, indicating that increased tumor cell proliferative rates resulting from perturbations in sleep may not be specific to a single cancerous cell type, and are potentially applicable to most solid tumors. Of note, the increased size of the tumors under SF conditions was also accompanied by more extensive and prominent areas of tumor core necrosis, further attesting to the changes in tumorigenesis elicited by the underlying SF. In parallel with the accelerated tumor expansion under SF conditions, increased tumor invasion to surrounding tissues was observed following both flank and thigh injections of TC-1 cells, with the latter thigh injections allowing for more accurate confirmation of the enhanced invasion process. Here again, multiple mechanisms have been described regarding the adaptive strategies that enable cell invasion across the physical outer boundaries of tumors. Therefore, an extensive and exhaustive survey of such mechanisms would be beyond the scope of current work. Notwithstanding, the unique clustering of TAM

in the periphery of SF-exposed tumors prompted us to explore whether such changes were potentially accountable for the more aggressive tumors during SF conditions. Indeed, the effects of alterations in TAM polarity and in innate immunity on tumor biological properties including growth trajectory and invasiveness to adjacent tissues have been extensively explored, and our current findings concur with such putative functions. (38-41) As indicated, the number of TAM was markedly increased in SF-exposed mice, and the differences were heterotopically distributed, with tumors from SF-exposed mice displaying preferential M2-type TAM localization in peripheral regions of the tumor. In contrast, SC-derived tumors had increased M1-type TAM, and these were located, in their greatest proportion within the core of the tumor. Therefore, we infer that the changes in macrophage polarity and location reflect some of the changes in tumor behavior. However, it remains unclear what mechanisms are operationally activated in the context of how SF elicits (i) a shift in TAM polarity within the tumor, or (ii) whether SF fosters increased migration of TAM from the circulation into the periphery. We should point out that the overall changes in TAM polarity were unexpected, particularly when considering the marked increases in M1 macrophage markers and in total numbers of macrophages that occur in visceral adipose tissues during SF (40). It is further possible that inflammatory changes in adipose tissues surrounding the tumors that resemble the changes in visceral white adipose tissue depots during SF may play a role in the shift of macrophages from the core to the periphery of the tumor, and further account for the M1/M2 phenotype shifts found here. Indeed, recent interest on the contribution of the adipose tissues surrounding tumors to tumor biological processes such as promotion of proliferation and invasion has recently emerged (43-45). Thus, altered sleep in the host may trigger a complex time-dependent cascade of activation and inactivation of biologically-relevant pathways both systemically and regionally (46), including peri-tumoral fat and intra-tumoral cellular substrates that cumulatively orchestrate changes in tumor growth and local invasiveness.

Similarly, the increased TLR4 expression in tumors excised from SF-exposed mice could either reflect selective migration of M2-TLR4+ TAM cells to these tumor regions from the systemic circulation, or changes in macrophage polarity, in macrophage TLR4 expression, or in migration of M1 from the core to the tumor periphery during SF. Accordingly, genetic ablation of TLR4 in mice resulted in major curtailment of not only tumor growth, but also of the differences between SF and SC. However, the SF-SC differences in tumor size persisted in either MYD88−/− and TRIF−/− mice, suggesting that either both TLR4 signaling pathways are required for SF-induced effect on tumor growth, or that the differences between SF and SC are not distinguishable once tumor growth is so markedly reduced by TLR4 genetic ablation. As with all other observations reported herein, transfer of the findings from an *in vivo* murine model to an *in vitro* model is obviously impossible, thereby hampering our ability to study mechanisms of SF effects in greater detail. We should also point out that the mechanisms underlying SF-induced activation of TLR4 signaling in macrophages, and the changes in TAM polarity are completely unknown, and this specific area will have to be explored in the future.

In summary, the present study conclusively demonstrates that perturbed sleep leads to major changes in tumorigenesis, characterized by increased tumor cell proliferation and invasion.

Alterations in TAM phenotypes, particularly in the tumor periphery, and in TLR4 expression in TAM further suggest that SF-induced effects on tumor growth and invasion may be mediated by host-related responses, particularly those involving innate immunity, and that improved understanding of such pathways may permit improved therapeutic interventions. Considering the high prevalence of sleep disorders and cancer in middle age or older populations, there are far reaching implications to current findings regarding potential adverse outcomes in patients in whom the 2 conditions co-exist.

Acknowledgments

Funding Sources: DG is supported by National Institutes of Health grants HL-065270 and HL-086662.

References

1. Abrams B. Cancer and sleep apnea--the hypoxia connection. Medical hypotheses. 2007; 68:232. [PubMed: 16905275]
2. Kripke DF, Garfinkel L, Wingard DL, Klauber MR, Marler MR. Mortality associated with sleep duration and insomnia. Archives of general psychiatry. 2002; 59:131–6. [PubMed: 11825133]
3. Verkasalo PK, Lillberg K, Stevens RG, Hublin C, Partinen M, Koskenvuo M, et al. Sleep duration and breast cancer: a prospective cohort study. Cancer research. 2005; 65:9595–600. [PubMed: 16230426]
4. Patel SR, Ayas NT, Malhotra MR, White DP, Schernhammer ES, Speizer FE, et al. A prospective study of sleep duration and mortality risk in women. Sleep. 2004; 27:440–4. [PubMed: 15164896]
5. Pinheiro SP, Schernhammer ES, Tworoger SS, Michels KB. A prospective study on habitual duration of sleep and incidence of breast cancer in a large cohort of women. Cancer research. 2006; 66:5521–5. [PubMed: 16707482]
6. Chung SA, Wolf TK, Shapiro CM. Sleep and health consequences of shift work in women. J Womens Health (Larchmt). 2009; 18:965–77. [PubMed: 19575690]
7. Gallicchio L, Kalesan B. Sleep duration and mortality: a systematic review and meta-analysis. Journal of sleep research. 2009; 18:148–58. [PubMed: 19645960]
8. Ikehara S, Iso H, Date C, Kikuchi S, Watanabe Y, Wada Y, et al. Association of sleep duration with mortality from cardiovascular disease and other causes for Japanese men and women: the JACC study. Sleep. 2009; 32:295–301. [PubMed: 19294949]
9. Kakizaki M, Kuriyama S, Sone T, Ohmori-Matsuda K, Hozawa A, Nakaya N, et al. Sleep duration and the risk of breast cancer: the Ohsaki Cohort Study. British journal of cancer. 2008; 99:1502–5. [PubMed: 18813313]
10. Kripke DF, Langer RD, Elliott JA, Klauber MR, Rex KM. Mortality related to actigraphic long and short sleep. Sleep medicine. 2011; 12:28–33. [PubMed: 20870457]
11. Liang JA, Sun LM, Muo CH, Sung FC, Chang SN, Kao CH. Non-apnea sleep disorders will increase subsequent liver cancer risk--a nationwide population-based cohort study. Sleep medicine. 2012; 13:869–74. [PubMed: 22503943]
12. McElroy JA, Newcomb PA, Titus-Ernstoff L, Trentham-Dietz A, Hampton JM, Egan KM. Duration of sleep and breast cancer risk in a large population-based case-control study. Journal of sleep research. 2006; 15:241–9. [PubMed: 16911025]
13. Sateia MJ, Lang BJ. Sleep and cancer: recent developments. Current oncology reports. 2008; 10:309–18. [PubMed: 18778557]
14. Thompson CL, Larkin EK, Patel S, Berger NA, Redline S, Li L. Short duration of sleep increases risk of colorectal adenoma. Cancer. 2011; 117:841–7. [PubMed: 20936662]
15. Tu X, Cai H, Gao YT, Wu X, Ji BT, Yang G, et al. Sleep duration and its correlates in middle-aged and elderly Chinese women: the Shanghai Women's Health Study. Sleep medicine. 2012; 13:1138–45. [PubMed: 22938861]

16. Jiao L, Duan Z, Sangi-Haghpeykar H, Hale L, White DL, El-Serag HB. Sleep duration and incidence of colorectal cancer in postmenopausal women. British journal of cancer. 2013; 108:213–21. [PubMed: 23287986]
17. Zhang X, Giovannucci EL, Wu K, Gao X, Hu F, Ogino S, et al. Associations of self-reported sleep duration and snoring with colorectal cancer risk in men and women. Sleep. 2013; 36:681–8. [PubMed: 23633750]
18. Savvidis C, Koutsilieris M. Circadian rhythm disruption in cancer biology. Mol Med. 2012; 18:1249–60. [PubMed: 22811066]
19. Sigurdardottir LG, Valdimarsdottir UA, Fall K, Rider JR, Lockley SW, Schernhammer E, Mucci LA. Circadian disruption, sleep loss, and prostate cancer risk: a systematic review of epidemiologic studies. Cancer Epidemiol Biomarkers Prev. 2012; 21:1002–11. [PubMed: 22564869]
20. Campos-Rodriguez F, Martinez-Garcia MA, Martinez M, Duran-Cantolla J, Pena Mde L, Masdeu MJ, et al. Association between obstructive sleep apnea and cancer incidence in a large multicenter Spanish cohort. American journal of respiratory and critical care medicine. 2013; 187:99–105. [PubMed: 23155146]
21. Nieto FJ, Peppard PE, Young T, Finn L, Hla KM, Farre R. Sleep-disordered breathing and cancer mortality: results from the Wisconsin Sleep Cohort Study. American journal of respiratory and critical care medicine. 2012; 186:190–4. [PubMed: 22610391]
22. Almendros I, Montserrat JM, Ramirez J, Torres M, Duran-Cantolla J, Navajas D, et al. Intermittent hypoxia enhances cancer progression in a mouse model of sleep apnoea. The European respiratory journal. 2012; 39:215–7. [PubMed: 22210813]
23. Almendros I, Montserrat JM, Torres M, Dalmases M, Cabanas ML, Campos-Rodriguez F, et al. Intermittent hypoxia increases melanoma metastasis to the lung in a mouse model of sleep apnea. Respiratory physiology & neurobiology. 2013; 186:303–7. [PubMed: 23499797]
24. Bhaskara VK, Mohanam I, Rao JS, Mohanam S. Intermittent hypoxia regulates stem-like characteristics and differentiation of neuroblastoma cells. PloS one. 2012; 7:e30905. [PubMed: 22363512]
25. Karoor V, Le M, Merrick D, Fagan KA, Dempsey EC, Miller YE. Alveolar hypoxia promotes murine lung tumor growth through a VEGFR-2/EGFR-dependent mechanism. Cancer Prev Res (Phila). 2012; 5:1061–71. [PubMed: 22700853]
26. Liu Y, Song X, Wang X, Wei L, Liu X, Yuan S, et al. Effect of chronic intermittent hypoxia on biological behavior and hypoxia-associated gene expression in lung cancer cells. Journal of cellular biochemistry. 2010; 111:554–63. [PubMed: 20568121]
27. Malec V, Gottschald OR, Li S, Rose F, Seeger W, Hanze J. HIF-1 alpha signaling is augmented during intermittent hypoxia by induction of the Nrf2 pathway in NOX1-expressing adenocarcinoma A549 cells. Free radical biology & medicine. 2010; 48:1626–35. [PubMed: 20347035]
28. Diers AR, Vayalil PK, Oliva CR, Griguer CE, Darley-Usmar V, Hurst DR, et al. Mitochondrial bioenergetics of metastatic breast cancer cells in response to dynamic changes in oxygen tension: effects of HIF-1alpha. PloS one. 2013; 8:e68348. [PubMed: 23840849]
29. Ramesh V, Nair D, Zhang SX, Hakim F, Kaushal N, Kayali F, et al. Disrupted sleep without sleep curtailment induces sleepiness and cognitive dysfunction via the tumor necrosis factor-alpha pathway. Journal of neuroinflammation. 2012; 9:91. [PubMed: 22578011]
30. Zhang SX, Khalyfa A, Wang Y, Carreras A, Hakim F, Neel BA, et al. Sleep fragmentation promotes NADPH oxidase 2-mediated adipose tissue inflammation leading to insulin resistance in mice. Int J Obes (Lond). 2013
31. Fukuda K, Kobayashi A, Watabe K. The role of tumor-associated macrophage in tumor progression. Front Biosci (Schol Ed. 2012; 4:787–98. [PubMed: 22202090]
32. Ruffell B, Affara NI, Coussens LM. Differential macrophage programming in the tumor microenvironment. Trends in immunology. 2012; 33:119–26. [PubMed: 22277903]
33. Kaushal N, Ramesh V, Gozal D. Human apolipoprotein E4 targeted replacement in mice reveals increased susceptibility to sleep disruption and intermittent hypoxia. American journal of physiology Regulatory, integrative and comparative physiology. 2012; 303:R19–29.

34. Gialeli C, Theocharis AD, Karamanos NK. Roles of matrix metalloproteinases in cancer progression and their pharmacological targeting. The FEBS journal. 2011; 278:16–27. [PubMed: 21087457]
35. Kessenbrock K, Plaks V, Werb Z. Matrix metalloproteinases: regulators of the tumor microenvironment. Cell. 2010; 141:52–67. [PubMed: 20371345]
36. Hua D, Liu MY, Cheng ZD, Qin XJ, Zhang HM, Chen Y, et al. Small interfering RNA-directed targeting of Toll-like receptor 4 inhibits human prostate cancer cell invasion, survival, and tumorigenicity. Molecular immunology. 2009; 46:2876–84. [PubMed: 19643479]
37. Yang H, Zhou H, Feng P, Zhou X, Wen H, Xie X, et al. Reduced expression of Toll-like receptor 4 inhibits human breast cancer cells proliferation and inflammatory cytokines secretion. Journal of experimental & clinical cancer research : CR. 2010; 29:92. [PubMed: 20618976]
38. Gajewski TF, Schreiber H, Fu YX. Innate and adaptive immune cells in the tumor microenvironment. Nature immunology. 2013; 14:1014–22. [PubMed: 24048123]
39. Green CE, Liu T, Montel V, Hsiao G, Lester RD, Subramaniam S, et al. Chemoattractant signaling between tumor cells and macrophages regulates cancer cell migration, metastasis and neovascularization. PloS one. 2009; 4:e6713. [PubMed: 19696929]
40. Obeid E, Nanda R, Fu YX, Olopade OI. The role of tumor-associated macrophages in breast cancer progression (review). International journal of oncology. 2013; 43:5–12. [PubMed: 23673510]
41. Takahashi T, Ibata M, Yu Z, Shikama Y, Endo Y, Miyauchi Y, et al. Rejection of intradermally injected syngeneic tumor cells from mice by specific elimination of tumor-associated macrophages with liposome-encapsulated dichloromethylene diphosphonate, followed by induction of CD11b(+)/CCR3(−)/Gr-1(−) cells cytotoxic against the tumor cells. Cancer immunology, immunotherapy : CII. 2009; 58:2011–23.
42. Wang Y, Carreras A, Lee S, Hakim F, Zhang SX, Nair D, et al. Chronic sleep fragmentation promotes obesity in young adult mice. Obesity (Silver Spring). 2013
43. Howe LR, Subbaramaiah K, Hudis CA, Dannenberg AJ. Molecular Pathways: Adipose Inflammation as a Mediator of Obesity-Associated Cancer. Clinical cancer research : an official journal of the American Association for Cancer Research. 2013
44. Nieman KM, Romero IL, Van Houten B, Lengyel E. Adipose tissue and adipocytes support tumorigenesis and metastasis. Biochimica et biophysica acta. 2013; 1831:1533–41. [PubMed: 23500888]
45. Wagner M, Dudley AC. A three-party alliance in solid tumors: Adipocytes, macrophages and vascular endothelial cells. Adipocyte. 2013; 2:67–73. [PubMed: 23805401]
46. Gharib SA, Khalyfa A, Abdelkarim A, Bhushan B, Gozal D. Integrative miRNA-mRNA profiling of adipose tissue unravels transcriptional circuits induced by sleep fragmentation. PloS one. 2012; 7:e37669. [PubMed: 22629440]

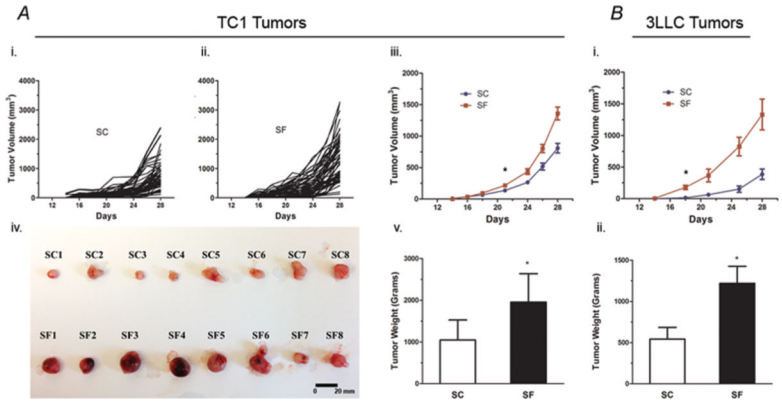

Figure 1. SF induces accelerated tumor size growth both in TC1 and 3LLC tumors

A. C57/B6 mice exposed to SF starting 1-week prior to flank injection with TC-1 cells showed accelerated tumor size growth and weight with significant differences when compared to mice under SC conditions. (i). shows the trajectory of tumor growth measured under SC conditions (n=53), compared to tumors from SF exposed mice; (ii). SF, n= 55.; (iii). When comparing the average tumor growth for both conditions, statistically significant differences emerged at day 23 following injection and sustained thereafter ($p< 0.007$). (iv) Macroscopic differences between the SF and SC tumors in samples of enucleated tumors. (v). Tumor weight was also significantly higher at day 28 in SF-exposed mice (SF-57/B6: 1.955± 0.680 g vs. SC-C57/B6: 1.046±0.479 g; $p<0.001$; n= 109 in each group). Of note, those experiments were performed in batches of 20 mice each, using the same tumor cell injection and follow-up protocols.

B. Mice (n=15/group) exposed to SF and injected with 3LLC cells showed significantly accelerated tumor growth compared to SC conditions, (i) with differences emerging after 19 days from cells injection ($p<0.001$), and (ii) significant tumor weight differences at enucleation (SF-57/B6: 1.22 ± 0.281 g vs. SC-C57/B6: 0.543 ±0.163 g; $p<0.027$). *$p< 0.05$

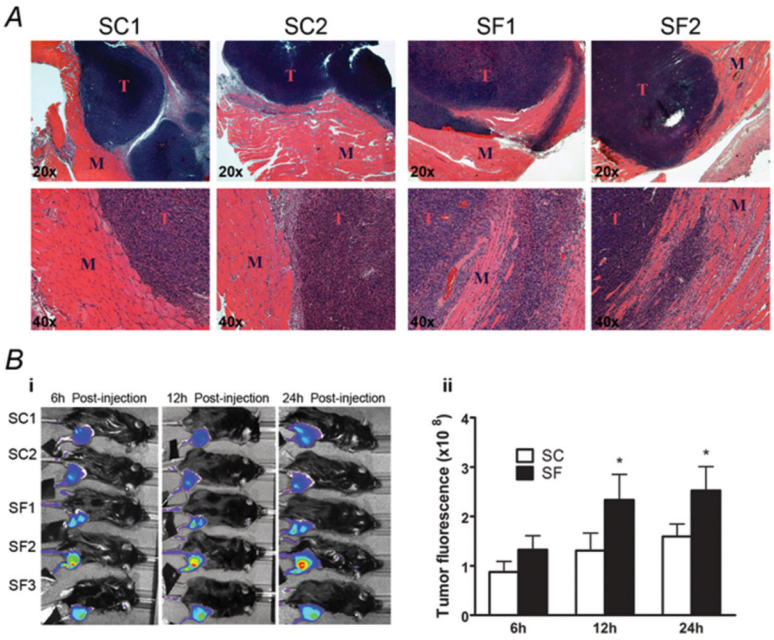

Figure 2. SF induces increased tumor invasiveness

A) Representative H&E sections of the TC1 tumors and the adjacent muscular tissue (cells were injected s.c. in the thigh area), increased invasiveness was apparent in SF-C57/B6 tumors compared to SC-C57/B6 conditions, with obvious penetration of surrounding tumor capsule and extension/infiltration into adjacent muscle. B) (i). Representative live MMP imaging (n=6/group) showing statistically significant increases in MMP activity in SF-C57/B6 tumors vs. CS-C57/B6. (ii). Significant differences in MMP activity continued to be apparent after 12 and 24h, with higher activity in SF vs. SC tumors. *p< 0.05

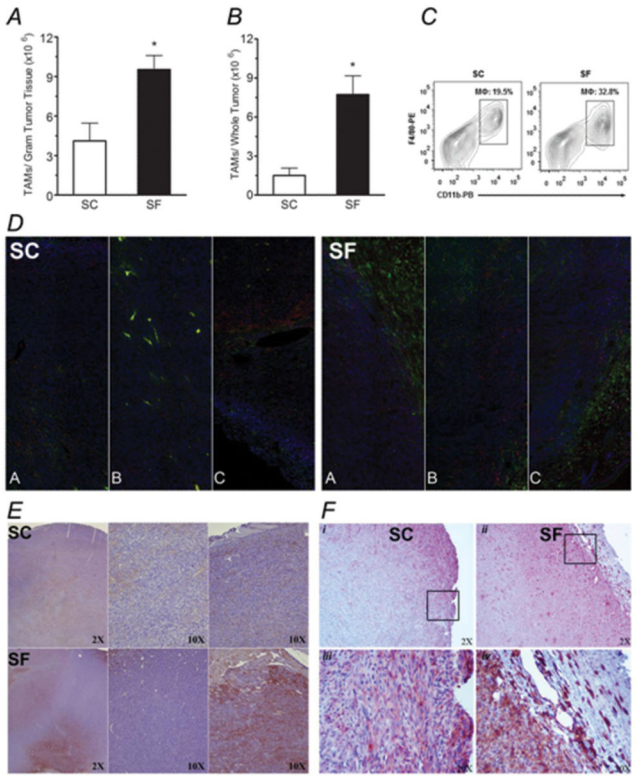

Figure 3. Tumor associated macrophage (TAM) counts and distribution

A) Significant increases in TAM counts in tumor tissue occurred in SF when compared with SC conditions (~3-fold increase). B) Almost 5-fold increase in TAM counts emerged when comparing the number of TAM/whole tumor in SF vs. SC. C) Representative FACS count of TAMS; CD45+, CD11b+, F4/80+ cells . D) Immunofluorescence imaging of whole tumor sections from both SF and SC conditions with images A and C representing both sides of the tumor capsule and B representing the tumor core; those images showing that TAM are preferentially distributed and in close proximity to the tumor capsule in SF conditions, while in SC conditions, increased tumor core location of TAM was found (n=6; Blue- Hoechst-Nuclei; Red-CD45+; Green- F4/80+). E) Representative tumor section stained with Hematoxilyn and F4/80+ illustrating a preferential distribution of TAM with more TAM in the tumor capsule in SF-exposed mice when compared to SC conditions (n=10; Brown-F4/80+ cells). F) Representative endocan stained sections showing higher immunoreactivity in the tumor capsule in SF conditions when compared to SC; this was apparent in low magnification (i, ii), as well as at higher magnification (iii; iv)(n=6; Brown- Endocan). *p< 0.05

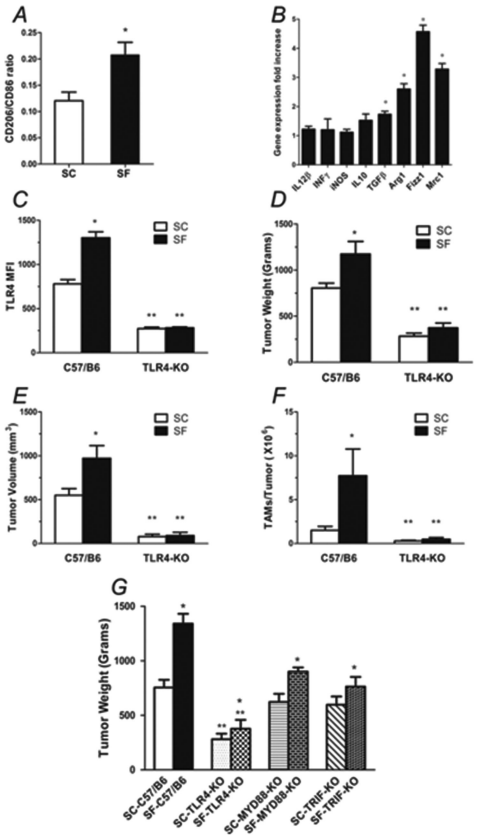

Figure 4. TAM polarity and TLR4 signaling

A) TAM (CD45+ CD11b+ F4/80+) flow cytometric assessment for the proportion of CD 86^{high}, a M1 marker or CD 206^{high}, a M2 marker, showing a shift toward increased M2 marker expression in TAM of SF-C57/B6 tumors (n=6). B) RT-PCR gene expression analysis of TAM, showed a shift in polarity in SF tumors with higher expression of M2 markers (Fizz1, Arg1 and Mrc1) when compared to SC conditions (n=6). C) TAM from SF-exposed mice expressed higher levels of TLR4 compared to SC-exposed mice (n=6). D&E) SC-TLR4−/− mice injected with TC1 tumor cells had a significantly reduced tumor weight and size when compared to SC-C57/B6 mice (n= 20/ group). Moreover, the accelerated growth and increased size induced by SF exposures were completely abrogated in SF-TLR4−/− mice (n=20). F) FACS assessment of TAM (CD45+ CD11b+ F4/80+) counts in tumors from TLR4−/− compared with C57/B6 conditions shows complete abrogation of the effect of SF, with significant reductions in TAM count in SF-TLR4−/− mice (n=20). G) Tumors weight at enucleation after 28 days of TC1 tumor cells injection in C57/B6 wild type, TLR4−/−, MYD88−/− and TRIF−/− mice, shows that tumors in SF-MYD88−/− and SF-TRIF−/− mice had reduced tumor weight compared to SF-C57/B6, but still significantly larger than in SF-TLR4−/− mice (n=12/group). In addition, small, albeit statistically significant differences between SF and SC for MYD88 and TRIF null mice remained. *p< 0.05 when comparing SC vs. SF conditions; **p<0.05 when comparing different strains.